2010 IEEE International Conference on Robotics and Automation
Anchorage Convention District
May 3-8, 2010, Anchorage, Alaska, USA

Circulation of curves using vector fields: actual robot experiments in 2D and 3D workspaces

Vinícius M. Gonçalves, Luciano C. A. Pimenta, Carlos A. Maia, Guilherme A. S. Pereira, Bruno C. O. Dutra, Nathan Michael, Jonathan Fink, and Vijay Kumar

Abstract— **Different robotic tasks can be solved by controlling a robot to circulate along curves. These include, for example, border inspection and surveillance, multirobot manipulation, and pattern generation. In a previous, work we have proposed a vector field approach for robot convergence and circulation along time-varying curves embedded in N-dimensional spaces. In the present work we instantiate this approach for three-dimensional spaces and, for the first time, show the efficacy of this method to control actual robots. Besides new theoretical analysis when constant speed control is applied, we present experimental results with aerial (quadrotors) and ground (differential-driven) robots.**

I. Introduction

Recently, the problem of controlling a robot to converge to and circulate along closed curves has drawn the attention of several researchers. Different tasks, such as surveillance, manipulation, and boundary monitoring can be executed by means of solutions of this problem. A very interesting application is shown for instance in [1], in which a group of aerial vehicles is used to pursue and circulate a chemical cloud that was released in the atmosphere.

In [2], [3] and [4], vector fields were used to solve the pattern generation problem, in which large groups of robots must converge to a specific curve in the plane. The main difference among the works is the way these fields are computed. The authors of [2] and [3] have computed the attractive field as the gradient of a function given by the interpolation of several radial basis functions centered at samples of the desired pattern. On the other hand, the authors of [4] have proposed to use a numerical method to compute, in an efficient way, an electrostatic field to attract a group of robots to a given target curve. The main advantage of their approach was the possibility to use the method in workspaces with obstacles. Artificial vector fields are particularly interesting due to the robustness of such methods to localization and actuator errors, which allows for real world applications, and the possibility to integrate planning and control in the same approach.

V. M. Gonçalves, C. A. Maia, G. A. S. Pereira, and B. C. O. Dutra are with the Department of Electrical Engineering, Universidade Federal de Minas Gerais, Belo Horizonte, MG, 31270-901, Brazil. {mariano, maia, gpereira}@cpdee.ufmg.br, brunocodutra@gmail.com

L. C. A. Pimenta is with the Department of Electronic Engineering, Universidade Federal de Minas Gerais, Belo Horizonte, MG, 31270-901, Brazil. lucpim@cpdee.ufmg.br

N. Michael, J. Fink and V. Kumar are with the GRASP Laboratory, University of Pennsylvania, Philadelphia, PA 19104, USA. {nmichael, jonfink, kumar}@grasp.upenn.edu

In some previous works, the robots were only attracted to the target curve, in which they should remain in a static configuration. However, for some problems it is also necessary another vector field to enforce the robots to circulate along the curve. In the case of a fixed-wing UAV (Unmanned Air Vehicle), for example, the robot must maintain a minimum speed and cannot converge to a single point. Therefore most of the tasks to be accomplished for this kind of robots must be modeled as a problem of convergence and circulation of curves. In this sense, for instance, [5] have controlled a UAV to track a moving target by using a vector field that guide it to a circle centered on the target. The composition of an attractive and a rotational field usually can be used to create an attractive limit cycle in the robot configuration space. Besides this paper, this idea was also used in [6], [7], [5], [8], [9], [10], and [11].

Some vector field based approaches, such as [12], consider N-dimensional spaces. However, most solutions that generate vector fields for curve tracking assume two-dimensional spaces. An exception is our previous work [13], in which time-varying curves in N-dimensional spaces are considered. In that paper it is presented the theory of the methodology, formal proofs of convergence, and simple numerical simulations. All results assumed the simple holonomic, kinematic model:

$$\dot{\mathbf{q}} = \mathbf{u}\,, \tag{1}$$

where $\dot{\mathbf{q}}$ is the robot velocity and $\mathbf{u}$ is the control input vector.

The present paper intends to show that our previous results can be applied to control real mobile robots. We present: (i) further analyses of the controller proposed in [13]; and (ii) experimental results with ground and aerial robots.

This paper is organized as follows. In Section II we present a general methodology to generate an artificial vector field for guiding a robot towards a given curve and circulate along this curve. In Section III we show some experimental results with actual robots in 2D and 3D workspaces. Finally, we present our conclusions and discuss future directions in Section IV.

II. Methodology

In [13] the authors proposed a methodology to converge to and circulate along a desired curve embedded in N-dimensional space. Furthermore, the curve can be static or time varying. In this section we review the methodology assuming three dimensional spaces (as the experimental

results presented in this paper deal with this case), which is a particular case of the main result in [13]. Afterwards, we present a novel analysis of the proposed controller in the case of time-varying curves.

A. Vector fields for 3D spaces

Before we start, we need to discuss some definitions. Unless mentioned otherwise, all the vectors considered in the paper are column vectors, $\mathbf{q} = [x \;\; y \;\; z]^T$, and ∇ is the gradient with respect to the coordinates x, y, z.

The proposed methodology is based on the existence of two functions α_1 and α_2, such that the desired curve is obtained by the intersection of the zero level set of such functions. Let $\mathcal{D}(t)$ be the set of points $\mathbf{q}$ such that at time t the functions α_1 and α_2 vanish. Thus, under certain constraints imposed on the functions α_i, the set $\mathcal{D}(t)$ is a one-dimensional set embedded in $\mathbb{R}^3$. Figure 1 illustrates this idea. Figure 2 presents ideal simulation results which illustrates our objective: a robot must converge to and circulate along the target set $\mathcal{D}(t)$ from every initial condition. We assume the robot kinematic model in (1).

We will first assume that the target set $\mathcal{D}(t)$ is static. In order to achieve convergence, we use a function $V(\alpha_1, \alpha_2)$: a negative definite function with continuous partial derivatives, such that its gradient is null only at the origin. The control law for convergence is given by:

$$\mathbf{u} = G\,\nabla V\,, \tag{2}$$

where G is a non null positive function, and the vector $G\nabla V$ points toward the set of points such that $\nabla V = \mathbf{0}$, which include the set $\mathcal{D}(t)$, where $\alpha_1 = 0$ and $\alpha_2 = 0$, since V is a negative definite differentiable function. If the remaining points where $\nabla V = \mathbf{0}$ are not attraction points to the system then convergence is guaranteed.

If $\mathcal{D}(t)$ is time varying, it is necessary to add a component to compensate the time variation of the curve. Let the functions $\alpha_1(x, y, z, t)$ and $\alpha_2(x, y, z, t)$ be differentiable functions, and let $M(\alpha)$ be the $\mathbb{R}^{3\times 3}$ matrix

$$M(\alpha) = \begin{bmatrix} \nabla\alpha_1^T \\ \nabla\alpha_2^T \\ (\nabla\alpha_1 \times \nabla\alpha_2)^T \end{bmatrix}, \tag{3}$$

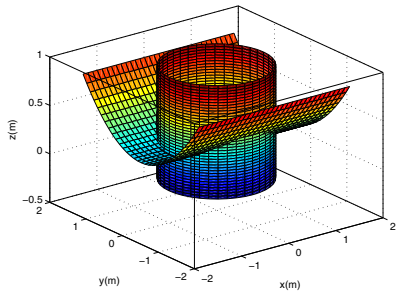

Fig. 1. Intersection of two surfaces $\alpha_1 = 0$ and $\alpha_2 = 0$: the set $\mathcal{D}(t)$ (in this case, static).

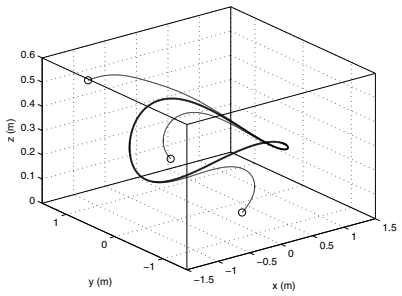

Fig. 2. Simulations for the target curve, given by the intersection of the two surfaces in Figure 1. The circles represent several initial robot configurations.

where $\times$ is the vector cross product operator. Also, consider the vector

$$\mathbf{a}(\alpha) = \left[\frac{\partial\alpha_1}{\partial t} \;\; \frac{\partial\alpha_2}{\partial t} \;\; 0\right]^T. \tag{4}$$

The desired component can be given by $-M(\alpha)^{-1}\mathbf{a}(\alpha)$. By adding this term to the right side of (2) convergence is guaranteed to time-varying curves. A further analysis about the influence of this term will be given in Section II-B.

Now, we will address the problem of circulation. Assume again that the curve is static and that the system has already converged to the desired curve. The vectors $\nabla\alpha_1$ and $\nabla\alpha_2$ are orthogonal to, respectively, the level sets of α_1 and α_2. Since the desired curve is the intersection of two particular level sets (zero level sets) then, at a point $\mathbf{q}$ in the desired curve, the vectors $\nabla\alpha_1$ and $\nabla\alpha_2$ are orthogonal to a vector which is tangent to the curve at this point. Provided that the gradient vectors are linearly independent, there is only one vector (up to a scale) that is orthogonal to both vectors: the cross product $\nabla\alpha_1 \times \nabla\alpha_2$. Therefore, the following control law guarantees circulation:

$$\mathbf{u} = H\,\nabla\alpha_1 \times \nabla\alpha_2\,, \tag{5}$$

where H is a non null function. The sign of H on the desired curve defines the direction of circulation.

As in the case of simple convergence, if the curve is time varying it is necessary to add a term to the right side of (5). It turns out that the same term can be used for circulation: $-M(\alpha)^{-1}\mathbf{a}(\alpha)$.

To achieve both convergence and circulation simultaneously, we can combine Equations (2) and (5), together with the correction term. Convergence and circulation are independent, *i.e.* they do not interfere with each other, because the vectors ∇V and $\nabla\alpha_1 \times \nabla\alpha_2$ are orthogonal. By the chain rule, ∇V is a linear combination of $\nabla\alpha_1$ and $\nabla\alpha_2$, and $\nabla\alpha_1 \times \nabla\alpha_2$ is orthogonal to both vectors. Therefore, merging the equations

$$\mathbf{u} = G\nabla V + H\nabla\alpha_1 \times \nabla\alpha_2 - M(\alpha)^{-1}\mathbf{a}(\alpha). \tag{6}$$

This control law guarantees convergence and circulation, which is our objective. The technical features and the formal proof of this fact can be found in [13].

B. Further Analysis of the Proposed Controller

In this section we will point out the importance of the correction term $(-M(\alpha)^{-1}\mathbf{a}(\alpha))$ to the controller in (6). Before we proceed, the following definition will be useful.

Definition 1 *The induced pseudo-inferior norm of a matrix $A \in \mathbb{R}^{m\times n}$, $\|A\|_{inf}$ is defined as*

$$\|A\|_{inf} = \min_{\mathbf{x}\neq\mathbf{0}} \frac{\|A\mathbf{x}\|}{\|\mathbf{x}\|}, \tag{7}$$

where $\mathbf{x} \in \mathbb{R}^n$ and $\|.\|$ is a vector norm. If the norm is the usual Euclidean norm (the case in this paper) then

$$\|A\|_{inf} = \sqrt{\lambda_{min}(A^TA)}, \tag{8}$$

where $\lambda_{min}(A^TA)$ is the minimum eigenvalue of A^TA.

Remark 1 *The denomination "norm" is a misnomer since the operator $\|\cdot\|_{inf}$ violates the triangle inequality. With this in mind, it is called pseudo norm because there are non null matrices A such that $\|A\|_{inf}$ vanishes. If the row rank of A is less than the number of columns then $\|A\|_{inf} = 0$.*

An interesting property of our pseudo norm is given next.

Property 1 *For a matrix A and vector $\mathbf{x}$ of appropriate dimensions*

$$\|A\mathbf{x}\| \geq \|A\|_{inf}\|\mathbf{x}\|. \tag{9}$$

Proof: This property comes directly from the definition in (7). For any vector $\mathbf{x}$ we have:

$$\|A\|_{inf} \leq \frac{\|A\mathbf{x}\|}{\|\mathbf{x}\|}. \tag{10}$$

■

As presented in the last section, the proposed controller is composed by three terms: one for convergence, one for circulation and one for correction in the case of time-varying curves. A natural question to ask is how relevant this correction term is and what are the implications of removing it.

Assume constant speed ($\|\dot{\mathbf{q}}\|$ = constant) and bounded time-derivative of the curve, which are reasonable assumptions for actual robots and real world tasks (see [14], for example). Consider also the definitions:

Definition 2 *A time-varying set of points, $\mathcal{S}(t)$, of a dynamical system $\dot{\mathbf{q}} = \mathbf{h}(\mathbf{q}, t)$ is said to be a repulsive set if there exists a neighborhood $\mathcal{N}(\mathcal{S})$ such that for all $\mathbf{q} \in \mathcal{N}$ we have $\dot{D} > 0$ for all t, where D is the distance between $\mathbf{q}$ and $\mathcal{S}$.*

$$M_*(\alpha) = \begin{bmatrix} \nabla\alpha_1^T \\ \nabla\alpha_2^T \end{bmatrix}, \tag{11}$$

$$\mathbf{a}_*(\alpha) = \begin{bmatrix} \frac{\partial\alpha_1}{\partial t} & \frac{\partial\alpha_2}{\partial t} \end{bmatrix}^T. \tag{12}$$

We will now show that removing the time varying correction term will cause a configuration steady-state error.

Theorem 1 *Let*

$$\mathbf{u} = v_r(G\nabla V + H(\nabla\alpha_1 \times \nabla\alpha_2)) \tag{13}$$

be a special case of the controller in (6), with $G = g(V)/\|\nabla V\|$ and $H = h(V)/\|\nabla\alpha_1 \times \nabla\alpha_2\|$ such that $g^2+h^2 = 1$. Therefore $\|\dot{\mathbf{q}}\| = v_r$. Assume also that $g(0) = 0$ and

$$\lim_{\mathbf{q}\to\mathcal{D}(t)} g(V)\frac{\nabla V}{\|\nabla V\|} = \mathbf{0}, \tag{14}$$

and ∇V can vanish on the desired set. If the variation of the curve is bounded in the sense that for all $\mathbf{q}$ and t $\|\mathbf{a}_*(\alpha)\| \leq v_c$ and $\|M_*(\alpha)^T\|_{inf} \geq v_{grad}$, and also the set of points such that $\nabla\alpha_i$'s are linearly dependent, $\mathcal{C}(t)$, is repulsive, then the system approaches the desired set $\mathcal{D}(t)$ when in the region

$$\mathcal{E}(t) = \{\mathbf{q}|\ g(V) > \frac{v_c}{v_{grad}v_r}\}. \tag{15}$$

Proof: By using the positive definite function $f = -V$, after simplifications, we have

$$\dot{f} = -v_r g\|\nabla V\| - \frac{\partial V}{\partial t}. \tag{16}$$

We will now prove that $\dot{f} < 0$ in $\mathcal{E}(t)$. One can note that $-g\|\nabla V\| \leq 0$, so, if $v_r g\|\nabla V\| \geq |\partial V/\partial t|$ then $\dot{f} < 0$. Let $\nabla_\alpha V$ be the gradient of V taken with respect to the external variables α_i. Thus,

$$\begin{aligned} v_r g\|\nabla V\| &= v_r g\|M_*(\alpha)^T\nabla_\alpha V\| && (17)\\ &\geq v_r g\|M_*(\alpha)^T\|_{inf}\|\nabla_\alpha V\|, && (18)\end{aligned}$$

by using Property 1. Applying also the fact that $\|M_*(\alpha)^T\|_{inf} \geq v_{grad}$

$$v_r g\|\nabla V\| \geq v_r v_{grad}\|\nabla_\alpha V\|. \tag{19}$$

Also, one can note that

$$\left|\frac{\partial V}{\partial t}\right| = |\nabla_\alpha V^T\mathbf{a}_*(\alpha)| \leq \|\mathbf{a}_*(\alpha)\|\|\nabla_\alpha V\|. \tag{20}$$

Since $\|\mathbf{a}_*(\alpha)\| \leq v_c$

$$\left|\frac{\partial V}{\partial t}\right| \leq v_c\|\nabla_\alpha V\|. \tag{21}$$

Therefore, if $v_r v_{grad}\|\nabla_\alpha V\| > v_c\|\nabla_\alpha V\|$ we can assure that $\dot{f} < 0$. Obviously, this inequality holds on the set $\mathcal{E}(t)$.

Since all equilibrium points (points such that $\nabla V = \mathbf{0}$, outside the desired curve) are in $\mathcal{C}(t)$ and by hypothesis this set is repulsive, then in the region $\mathcal{E}(t)$, the system approaches the desired curve $V = 0$.

■

We will discuss the implication of this theorem with an example. Consider a circle moving in $\mathbb{R}^3$, with time dependent radius described by the function $R(t)$, time dependent center described by the vector $\mathbf{q}_c(t) = [x_c(t)\ y_c(t)\ z_c(t)]^T$, and parallel to the plane $z = 0$. Also, let $\tilde{\mathbf{q}}$ be the vector

$[x\ y]^T$ and $\tilde{\mathbf{q}}_c$ be the vector $[x_c(t)\ y_c(t)]^T$. The following functions describe the circle:

$$\alpha_1 = \sqrt{(x - x_c(t))^2 + (y - y_c(t))^2} - R(t) = 0\,, \quad (22)$$

$$\alpha_2 = z - z_c(t) = 0. \quad (23)$$

Remark 2 *The set of points such that the vector $\nabla\alpha_1 \times \nabla\alpha_2$ vanishes is the set of points $[x_c(t)\ y_c(t)\ s]^T$ for any $s \in \mathbb{R}$. In our previous work [13] we present a very similar example where we show that this set is repulsive.*

Assume that $\|\dot{\tilde{\mathbf{q}}}_c\| \leq v_1$, $|\dot{R}(t)| \leq v_2$, and $|\dot{z}_c| < v_3$. Thus,

$$\left|\frac{\partial\alpha_1}{\partial t}\right| = \left|-\frac{(\tilde{\mathbf{q}} - \tilde{\mathbf{q}}_c)^T\dot{\tilde{q}}_c}{\|\tilde{\mathbf{q}} - \tilde{\mathbf{q}}_c\|} - \dot{R}(t)\right|, \quad (24)$$

and

$$\left|-\frac{(\tilde{\mathbf{q}} - \tilde{\mathbf{q}}_c)^T\dot{\tilde{q}}_c}{\|\tilde{\mathbf{q}} - \tilde{\mathbf{q}}_c\|} - \dot{R}(t)\right| \leq \|\dot{\tilde{q}}_c\| + |\dot{R}(t)| \leq v_1 + v_2. \quad (25)$$

Also,

$$\left|\frac{\partial\alpha_2}{\partial t}\right| = |-\dot{z}_c(t)| \leq v_3. \quad (26)$$

Therefore,

$$\|\mathbf{a}_*(\alpha)\| \leq \sqrt{(v_1 + v_2)^2 + v_3^2} = v_c\,, \quad (27)$$

which means that the time variation of the curve is bounded.

Assume that the controller in (13) is used. Also, lets choose $V = -\sqrt{\alpha_1^2 + \alpha_2^2}$ and $g(V) = -V/\sqrt{V^2 + 1}$. Now, we will bound $\|M_*(\alpha)^T\|_{inf}$ from below.

It is clear that $\nabla\alpha_1$ is orthogonal to $\nabla\alpha_2$ and $\|\nabla\alpha_1\| = \|\nabla\alpha_2\| = 1$. Therefore $M_*(\alpha)M_*(\alpha)^T$ is the 2×2 identity matrix and clearly $\|M_*(\alpha)^T\|_{inf} = 1$. This implies that the highest v_{grad} possible is $v_{grad} = 1$.

By Theorem 1 we know that once in the set

$$\mathcal{E}(t) = \left\{\mathbf{q} \mid v_r\frac{-V}{\sqrt{V^2 + 1}} \geq v_c\right\}, \quad (28)$$

the system approaches the desired curve. It should be clear that $v_c/v_r = v_{rel}$ must be less than 1 to $\mathcal{E}(t)$ not be empty. Therefore,

$$\mathcal{E}(t) = \left\{\mathbf{q} \mid -V \geq \frac{v_{rel}}{\sqrt{1 - v_{rel}^2}}\right\}. \quad (29)$$

Let $\Omega = v_{rel}/\sqrt{1 - v_{rel}^2}$. Thus, the set $\mathcal{E}(t)$ is the set of points $\mathbf{q}$ such that, at time t,

$$\left[\sqrt{(x - x_c)^2 + (y - y_c)^2} - R\right]^2 + (z - z_c)^2 \geq \Omega^2. \quad (30)$$

This set is precisely the complement on $\mathbb{R}^3$ of the interior of a torus surrounding the desired curve, with radius Ω. This radius provides then the upper bound on the error when we use the controller without the correction term. As v_{rel} decreases (the robot becomes "faster"), the error Ω also decreases.

To illustrate the previous discussion, we simulated the system with $R(t) = 2 + sin(t)$ and $\mathbf{q}_c = [0\ 0\ t]^T$. Therefore,

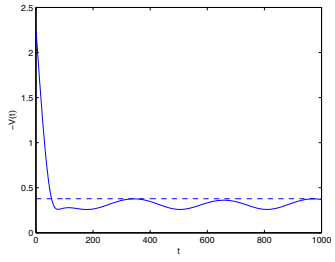

Fig. 3. Plot of $-V$ versus t. Since the correction term is not used, there is an error. The maximum theoretical error is shown in the picture as a dashed line, and it is practically the same of the simulated one.

(a) (b)

Fig. 4. Pictures of the robots: iRobot's Create (Fig. 4(a)) and quadrotor robot (Fig. 4(b)).

$v_c = \sqrt{2}$ (since $v_1 = 0$, $v_2 = 1$ and $v_3 = 1$) bounds the time variation. The initial condition is $x = y = 3, z = 0$. We set the robot speed to $v_r = 4$. According to our theory the maximum error on V must be $\Omega = 0.378$. Figure 3 plots $-V$ versus t and also (dashed) the theoretical bound. One can see that the simulated maximum error is practically equal to the theoretical value.

III. Experimental Results

To verify the proposed theory to control actual mobile robots, we have implemented the methodology in two different indoor platforms. The first one is composed by an iRobot's Create differential driven robot [15] (see Figure 4(a)) equipped with a Linux laptop and localized by an external visual system that is based on the ArtoolKitPlus Tracking Library. The second platform is constituted by an AscTec Hummingbird quadrotor [16] (see Figure 4(b)) from Ascending Technologies GmbH with an onboard Gumstix [17] computer localized by a Vicon tracking system [18]. Both platforms are programmed and simulated in C++ using the Player/Gazebo [19] environment. Movies are available at: http://coro.cpdee.ufmg.br/movies.

To control the Create robot to follow the vector field in Equation (6), we rely on the onboard velocity control system and used a kinematic, static feedback linearization controller that, basically, translates the field components to the robot's linear and angular velocities v and ω as:

$$\begin{bmatrix} v \\ \omega \end{bmatrix} = \begin{bmatrix} \cos\theta & \sin\theta \\ -\frac{\sin\theta}{d} & \frac{\cos\theta}{d} \end{bmatrix}\mathbf{u}\,, \quad (31)$$

where θ is the robot orientation and $d > 0$ defines a control point located at small distance from the robot center of mass. In this paper $d = 0.1$m.

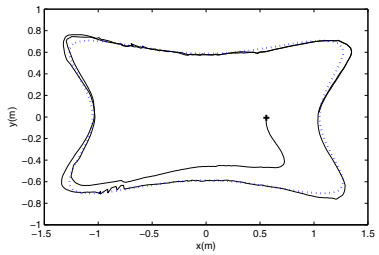

Fig. 5. Robot path (solid line) and desired static curve (dotted line).

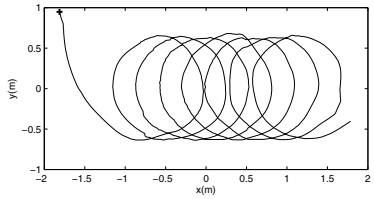

Fig. 6. Robot path when it is following a time-varying vector field determined by a moving circle.

Figure 5 shows the robot path as seen by the visual system when it is following a vector field determined by static functions of the form:

$$\alpha_1(x,y,z) = ax^4 - bx^2y^2 + cy^4 - 1$$
$$\alpha_2(x,y,z) = z\,,$$

where a, b, and c were chosen to fit the lab workspace. Not only for this experiment, but for all the experiments presented in this section, the negative definite function V was defined to be:

$$V = -\sqrt{\alpha_1^2 + \alpha_2^2}\,.$$

Notice in Figure 5 that some small localization noise do not prevent the robot to circulate the desired curve shown as dotted line. The difference between the robot path and the target curve can be explained by the distance d used in the feedback linearization controller.

In a second experiment with the Create robot it is possible to see that the vector field in Equation (6) can be used to track a time-varying curve. The time-varying curve in this case is a circle with constant radius and center moving in the x direction with 0.01m/s. The circle is obtained by intersecting a moving cylinder with the $z = 0$ plane. Notice that this curve may be tracked by the robot since its maximum speed is 0.5m/s. Figure 6 shows the robot path for this experiment while Figure 7 shows the behavior of $-V$ in function of time. Notice that $-V$ decreases very fast and, except for localization and actuation errors, remains very close to zero.

A second set of experiments was performed with a quadrotor robot. The quadrotor robot has a holonomic behaviour but, in order to follow the vector field in Equation (6), a dynamic controller is necessary to transform from the velocity components of the field to the control inputs required

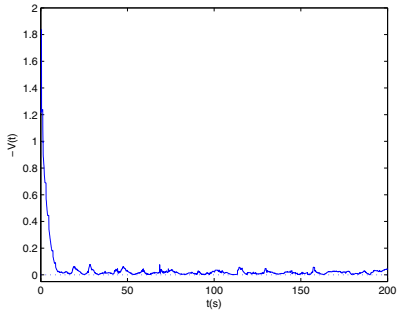

Fig. 7. Function $-V$ for the path in Figure 6.

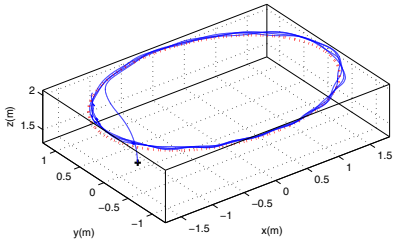

Fig. 8. Quadrotor path when it is following an ellipse parallel to the ground.

by the hardware platform. A complete description of this controller was previously published in [20]. Figure 8 shows an experiment where the quadrotor converges to a static ellipse parallel to the ground. This curve was obtained by the intersection of cylinder with an elliptic base with the plane $z = 2$m.

Another static vector field was computed to make the quadrotor robot circulate a saddle like curve. The robot path and the desired curve are shown in Figure 9. The functions for this experiment were defined as:

$$\alpha_1(x,y,z) = \left(\frac{x-x_c}{r_x}\right)^2 + \left(\frac{y-y_c}{r_y}\right)^2 - 1$$
$$\alpha_2(x,y,z) = z - z_{min} - (z_{max} - z_{min})\left(\frac{x-x_c}{r_x}\right)^2\,,$$

where $x_c = 0.0$m and $y_c = 0.0$m define the center of the curve in xy plane, $r_x = 1.75$m and $r_y = 1.25$m define the principal axes of the curve in the same plane and $z_{min} = 1$m and $z_{max} = 3$m limit the curve's z coordinate.

In our final experiment the quadrotor was controlled to track a time-varying curve represented by the intersection of a cylinder and a plane parallel to the ground with varying height. This plane was determined by a level set of the function $z - ((z_{max} - z_{min})(1 + cos(\omega t))/2 + z_{min})$, where z_{min} and z_{max} are defined as before, t is time, and $\omega = 0.1$ determines the height variation frequency. The robot path is shown in Figure 10. Figure 11 shows the behavior of $-V$ in function of time. Notice that once the robot converge to the curve, $-V$ remains very close to zero indicating that the robot is circulating the time-varying curve.

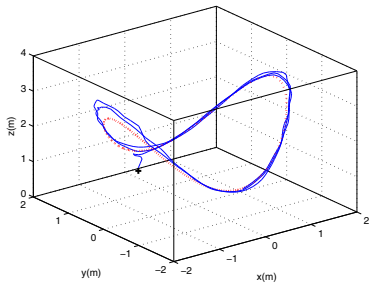

Fig. 9. Saddle like curve circulated by the quadrotor. The solid line represents the robot path and the dotted line the desired curve.

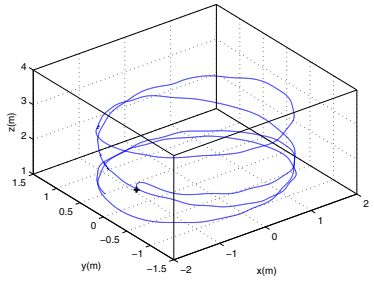

Fig. 10. Quadrotor path for a curve represented by a circle with a time varying center along the z axis.

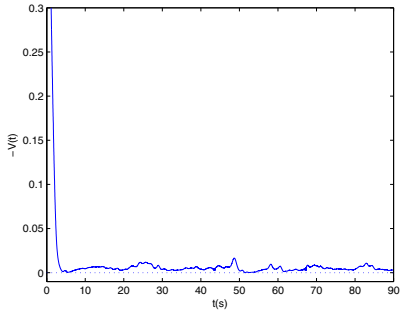

Fig. 11. Function $-V$ for the path in Figure 10.

IV. Conclusions and Future Work

This paper presents experimental results that validates the vector field proposed in [13] to control a ground and an aerial mobile robot to converge to and circulate along static and time-varying curves in two- and three-dimensional workspaces. By the authors knowledge, this is the first implementation of time-varying three-dimensional vector fields that controls actual aerial robots in such class of task. The proposed vector field is composed by a gradient term that is responsible to guide the robot to the curve, a curl term that makes the robot circulate along the curve, and feed-forward term that compensates the time-varying nature of the curve. In this paper we present a deep theoretical analysis of this field regarding the importance of the feed-forward term. Moreover, our theory gives bounds to the circulation and convergence errors when this term is not used and the variation of the curve and the robot speed are limited.

V. Acknowledgments

This work is part of the CNPq/NSF cooperation program, grant no 49.0743/2006-4. The authors gratefully acknowledge the support from FAPEMIG (Brazil), CNPq (Brazil), NSF grant no. IIS-0427313, ARO grant no. W911NF-05-1-0219, ONR grants no. N00014-07-1-0829 and N00014-08-1-0696, and ARL grant no. W911NF-08-2-0004.

References

[1] W. J. Pisano, D. A. Lawrence, and K. Mohseni, "Concentration gradient and information energy for decentralized uav control," in *AIAA Guidance, Navigation, and Control Conference and Exhibit*, 2006.

[2] L. Chaimowicz, N. Michael, and V. Kumar, "Controlling swarms of robots using interpolated implicit functions," in *Proceedings of the IEEE International Conference on Robotics Automation*, 2005, pp. 2498–2503.

[3] M. A. Hsieh and V. Kumar, "Pattern generation with multiple robots," in *Proceedings of the IEEE International Conference on Robotics and Automation*, 2006, pp. 2442–2447.

[4] L. C. A. Pimenta, M. L. Mendes, R. C. Mesquita, and G. A. S. Pereira, "Fluids in electrostatic fields: An analogy for multi-robot control," *IEEE Transactions on Magnetics*, vol. 43, pp. 1765–1768, 2007.

[5] E. W. Frew, D. A. Lawrence, C. Dixon, J. Elston, and W. J. Pisano, "Lyapunov guidance vector fields for unmanned aircraft applications," in *Proceedings of the American Control Conference*, 2007, pp. 371–376.

[6] M. Quigley, M. A. Goodrich, S. Griffiths, A. Eldredge, and R. Beard, "Target acquisition, localization, and surveillance using a fixed-wing mini-UAV and gimbaled camera," in *Proceedings of the IEEE International Conference on Robotics Automation*, 2005, pp. 2600–2605.

[7] M. A. Hsieh, S. Loizou, and V. Kumar, "Stabilization of multiple robots on stable orbits via local sensing," in *Proceedings of the IEEE International Conference on Robotics Automation*, 2007, pp. 2312–2317.

[8] F. Zhang and N. E. Leonard, "Coordinated patterns of unit speed particles on a closed curve," *Systems and Control Letters*, vol. 56, no. 6, pp. 397–407, 2007.

[9] N. Ceccarelli, M. D. Marco, and A. Giannitrapani, "Collective circular motion of multi-vehicle systems," *Automatica*, vol. 44, pp. 3025–3035, 2008.

[10] D. A. Lawrence, E. W. Frew, and W. J. Pisano, "Lyapunov vector fields for autonomous unmanned aircraft flight control," *Journal of Guidance, Control, and Dynamics*, vol. 31, no. 5, pp. 1220–1229, 2009.

[11] G. A. S. Pereira, D. R. Rebelo, P. Iscold, and L. A. B. Torres, "A vector field approach to guide small uavs through a sequence of waypoints," in *Anais do XVII Congresso Brasileiro de Automática (CBA'08)*, 2008.

[12] V. Gazi and K. M. Passino, "Stability analysis of social foraging swarms," *IEEE Transaction on Systems, Man, and Cybernetics—Part B: Cybernetics*, vol. 34, no. 1, pp. 539–557, 2004.

[13] V. G. Mariano, L. C. A. Pimenta, G. A. S. Pereira, and C. A. Maia, "Artificial vector fields for robot convergence and circulation of time-varying curves in n-dimensional spaces," in *Proceedings of the American Control Conference*, 2009, pp. 2012–2017.

[14] S. Waydo and R. M. Murray, "Vehicle motion planning using stream functions," in *Proceedings of the IEEE International Conference on Robotics Automation*, 2003, pp. 2484–2491.

[15] "irobot," http://store.irobot.com/, 2009.

[16] "Ascending Technologies, GmbH," http://www.asctec.de, 2009.

[17] "Gumstix," http://www.gumstix.com/, 2009.

[18] "Vicon Motion Systems, Inc," http://www.vicon.com, 2009.

[19] B. Gerkey, R. T. Vaughan, and A. Howard, "The player/stage project: Tools for multi-robot and distributed sensor systems," in *Proc. of the 11th Int'l. Conf. on Advanced Robotics*, 2003, pp. 317–323.

[20] N. Michael, J. Fink, and V. Kumar, "Cooperative manipulation and transportation with aerial robots," in *Proceedings of Robotics: Science and Systems*, Seattle, USA, June 2009.